

AVO modeling with non-zero phase spherical waves

Charles P. Ursenbach and Arnim B. Haase

ABSTRACT

Spherical-wave reflection coefficients are normally calculated using a zero-phase wavelet. The purpose of this study is to clarify whether phase affects reflectivity, and to explain the observed results. Numerical experiments show that zero-phase, rotated-phase, and linear-phase wavelets give identical reflectivities, but that minimum-phase wavelets give slightly different AVO results in a region beyond the critical angle, even though they share the same amplitude spectrum. Expressing the reflectivity calculation as a weighted integral of plane-wave coefficients provides insight into these results. The weighting functions for zero- and minimum-phase wavelets differ from each other. In particular, although the central part of the weighting does not differ appreciably, the edges differ significantly in ways that mimic the differences between reflection coefficient curves.

INTRODUCTION

Previous studies of spherical-wave AVO behavior (Haase, 2004) have shown the need for spherical-wave modeling near critical points. In these studies we have employed three different wavelets to date: Ormsby, Ricker, and Rayleigh. In all cases these were zero-phase, which is the simplest form of a wavelet, and is relevant to many cases of AVO modeling and inversion.

However, the question arises whether the phase has an influence on the reflectivity. Intuition might suggest that the calculated reflectivity is independent of phase because of two techniques employed in our methods: 1) The reflection coefficient is calculated from the envelope of the trace, so that *instantaneous* phase does not enter in. However, this does not necessarily proscribe a role for the spectral phase. 2) The reflection coefficient is normalized by the amplitude of a wave reflected in the same manner but with a plane-wave coefficient of unity. Thus phase contributions in the numerator and denominator could cancel; but strictly speaking this would only occur if they can be taken outside of integrals in both cases. If the phase is frequency dependent this would not be the case, so the question is reasonable to pose.

As described in this report, we approach the question as follows:

1. Develop a computer code for calculating spherical-wave reflection coefficients with non-zero phase wavelets.
2. Produce an appropriate set of test wavelets.
3. Produce reflection coefficient curves.
4. Analyze the results.

THEORY

As described elsewhere, a code developed by Haase (2004) calculates spherical-wave reflection coefficients by performing a numerical p -integration to obtain the ray-parallel displacement spectrum of Equation 1 at several frequency points:

$$U_{\parallel}(\omega) = \mathbf{r}_{\text{ray}} \cdot \nabla \phi(\omega) \quad (1a)$$

$$\phi(\omega) = A i \omega \exp(-i\omega t) \int_0^{\infty} \frac{p}{\xi_1} R_{\text{pp}}(p) J_0(\omega p r) \exp[i\omega \xi_1(z+h)] dp \quad (1b)$$

Here ω is the frequency, \mathbf{r}_{ray} is a unit vector in the ray direction at the receiver, ϕ is the spectrum of the displacement potential, A is an arbitrary scale factor, t is the time, p and ξ_1 are horizontal and vertical slownesses above the interface, R_{pp} is the plane-wave reflection coefficient, J_0 is a zeroth-order Bessel function, r is the source-receiver offset, and z and h are the vertical distances from the interface to the receiver and source.

Given the displacement spectrum, a time-trace can be obtained by multiplying by the wavelet spectrum and integrating over frequency, and from this trace the maximum of the envelope yields a reflectivity estimate. This is converted to a reflection coefficient by dividing by an estimate employing $R_{\text{pp}} = 1$.

The current program based on equation 1 was modified to accept complex-valued wavelet spectra.

We have previously put forward an alternate approach to calculating spherical-wave reflection coefficients (Ursenbach and Haase, 2004). This requires the use of Rayleigh wavelets and involves analytic integration over the frequency prior to the p -integration. The only phase forms which are consistent with this analytic integration are constant phase and linear phase. As shown below, these yield reflection coefficients identical to those obtained with zero-phase wavelets. Developing this type of program is therefore not of interest in the study of non-zero phase wavelets.

One result of the Rayleigh-wavelet approach is however useful here. The final result of that method is that spherical-wave reflection coefficients can be written

$$R_{\text{pp}}^{\text{spherical}}(\theta_i) = \int_{\Gamma} W(\theta, \theta_i; \text{wavelet}) R_{\text{pp}}(\theta) d(\cos \theta) \quad (2)$$

where θ_i is the angle of incidence, θ is an integration parameter [where $d(\cos \theta) = -\alpha_1(p/\xi_1)dp$, and α_1 is P-wave velocity above the interface], Γ is a complex integration path, and W is a normalized weighting function which depends on wavelet parameters. For Rayleigh wavelets W is an analytic function.

In principle, the spherical-wave reflection coefficient for any wavelet can be written in the form of equation 2. The only difference is that in general W is not known analytically. It can be represented numerically, though, and as this will be useful in our later analysis, we give the expression for this in equation 3 (derived in the appendix),

$$W = \frac{i \int_0^{\infty} w(\omega) \exp[-i\omega(R/\alpha_1 + t_{\text{shift}} - 2\xi_1 z)] [p \sin \theta_i J_1(\omega pr) - i\xi_1 \cos \theta_i J_0(\omega pr)] \omega^2 d\omega}{R^2 \alpha_1 \int_0^{\infty} w(\omega) \exp(-i\omega t_{\text{shift}}) (1 - iR\omega/\alpha_1) d\omega}, (3)$$

where w is the wavelet spectrum, $R \equiv \sqrt{r^2 + 4z^2}$ is the reflected ray distance from source to receiver, and t_{shift} is the time of the envelope maximum for a wavelet at $t = 0$ (i.e., $t_{\text{shift}} = 0$ for all zero-phase wavelets). Thus we have substituted t in equation 1b with the estimated time of arrival of the envelope maximum, namely $R/\alpha_1 + t_{\text{shift}}$.

As indicated above, equation 3 will assist in analyzing the results of this paper.

RESULTS

Equation 1 is applied to the calculation of spherical-wave reflection coefficients. All calculations are based on an earth model specified by the parameters in Table 1. The interface is defined to be 500 m below both the source and receiver. The only further information required for a calculation is a wavelet specification.

Table 1. Two-layer, elastic interface model employed in calculations.

	Density (kg/m ³)	P-wave velocity (m/s)	S-wave velocity (m/s)
Layer 1	2400	2000	879.88
Layer 2	2000	2933.33	1882.29

Six wavelets are employed for six different calculations. Four are Ormsby wavelets, each with a trapezoidal band defined by the parameters 5/15-80\100 Hz, and two are Rayleigh wavelets defined by the parameters $n = 4$ and $f_0 = 40$ Hz. In detail they are

1. Zero-phase Ormsby ($\phi(\omega) = 0^\circ$)
2. Constant-phase Ormsby ($\phi(\omega) = 60^\circ$)
3. Linear-phase Ormsby ($\phi(\omega) = \omega / 10\text{s}^{-1}$)
4. Minimum-phase Ormsby
5. Zero-phase Rayleigh
6. Minimum-phase Rayleigh

The constant- and linear-phase wavelets (2 and 3) are generated from zero-phase by multiplying the spectra by the necessary factors. The minimum-phase wavelets (4 and 6) are generated from their zero-phase analogues using the CREWES MATLAB toolbox routine **tommin**. The spectra of the wavelets, along with their amplitudes, are shown in Figure 1.

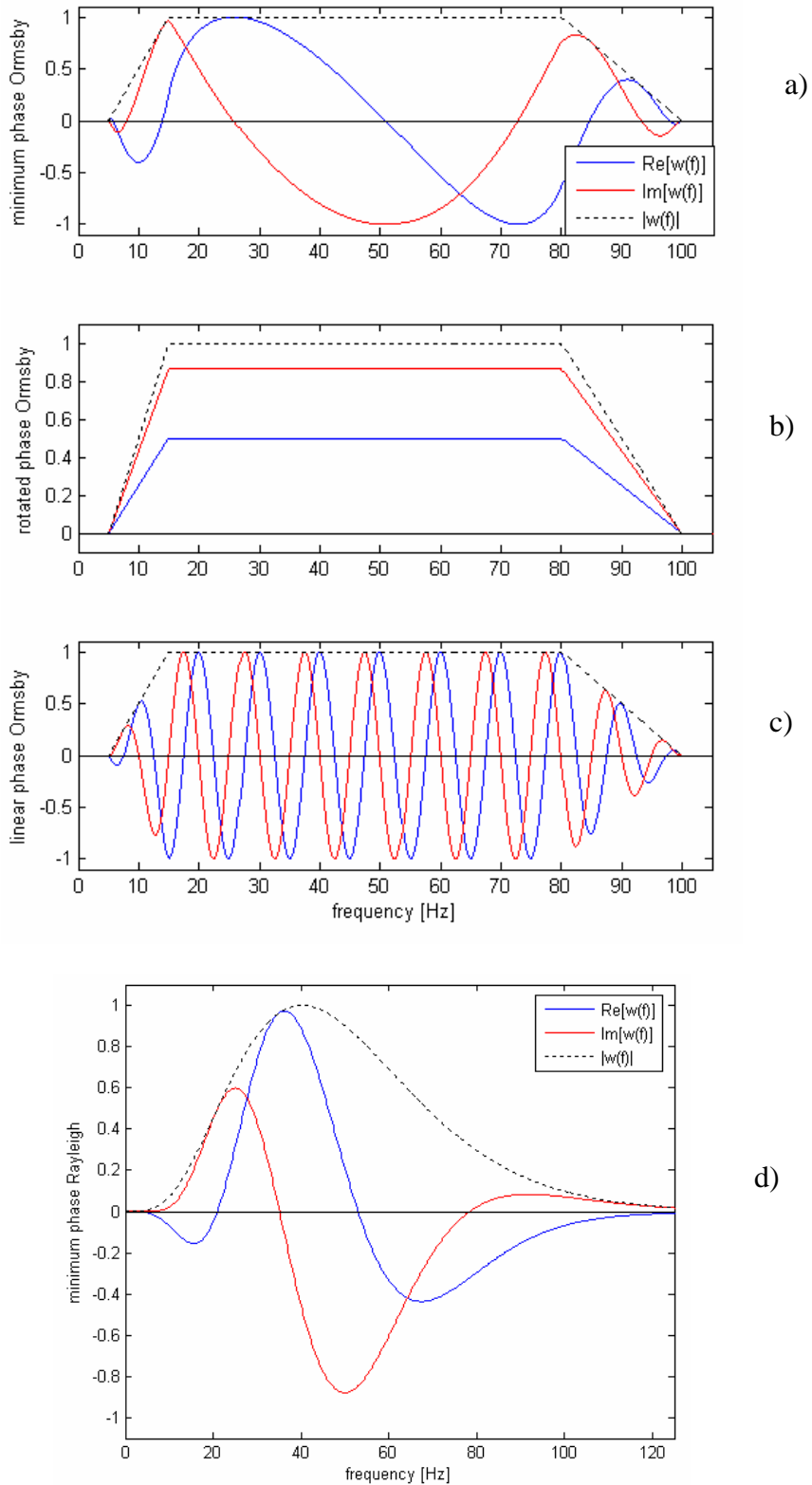


FIG. 1: The spectra of wavelets used in spherical-wave reflection coefficient calculations. The blue line shows the real part, the red the imaginary part, and the dotted black line the envelope (or zero-phase wavelet). In detail they are a) minimum-phase Ormsby, b) constant-phase Ormsby, c) linear-phase Ormsby, and d) minimum-phase Rayleigh.

In Figure 2 we compare the four spherical-wave reflection coefficients resulting from use of wavelets 1 through 4. Not all lines are visible, and this is because the results for zero-, constant- and linear-phase wavelets are identical. The result for the minimum-phase wavelet is somewhat different however. The ripples typically seen in the post-critical region for the zero-phase wavelet are now absent, and instead there is a smooth approach to the plane-wave result.

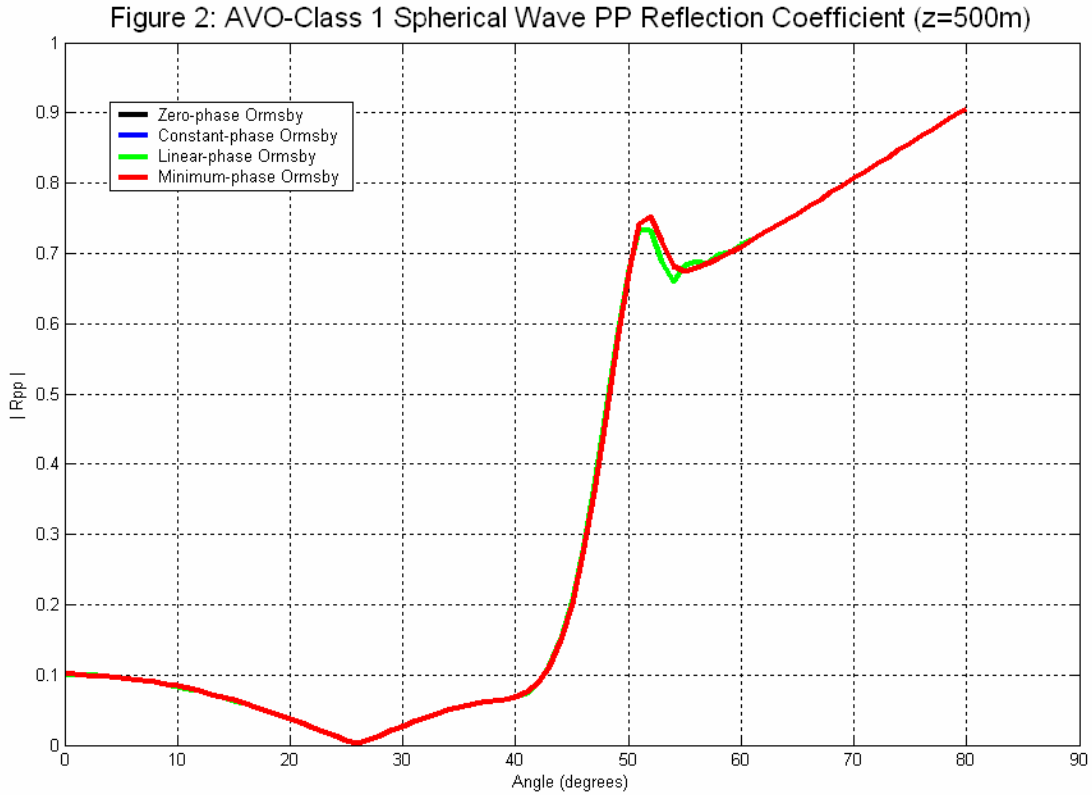


FIG. 2: Spherical-wave reflection coefficient curves for four different Ormsby wavelets which share the same amplitude spectrum but differ in phase. The blue and black curves are identical to and hidden by the green line.

In Figure 3 we compare the two Rayleigh wavelet results. In this case the zero-phase wavelet does not produce oscillatory post-critical behavior, but differences still exist in this region.

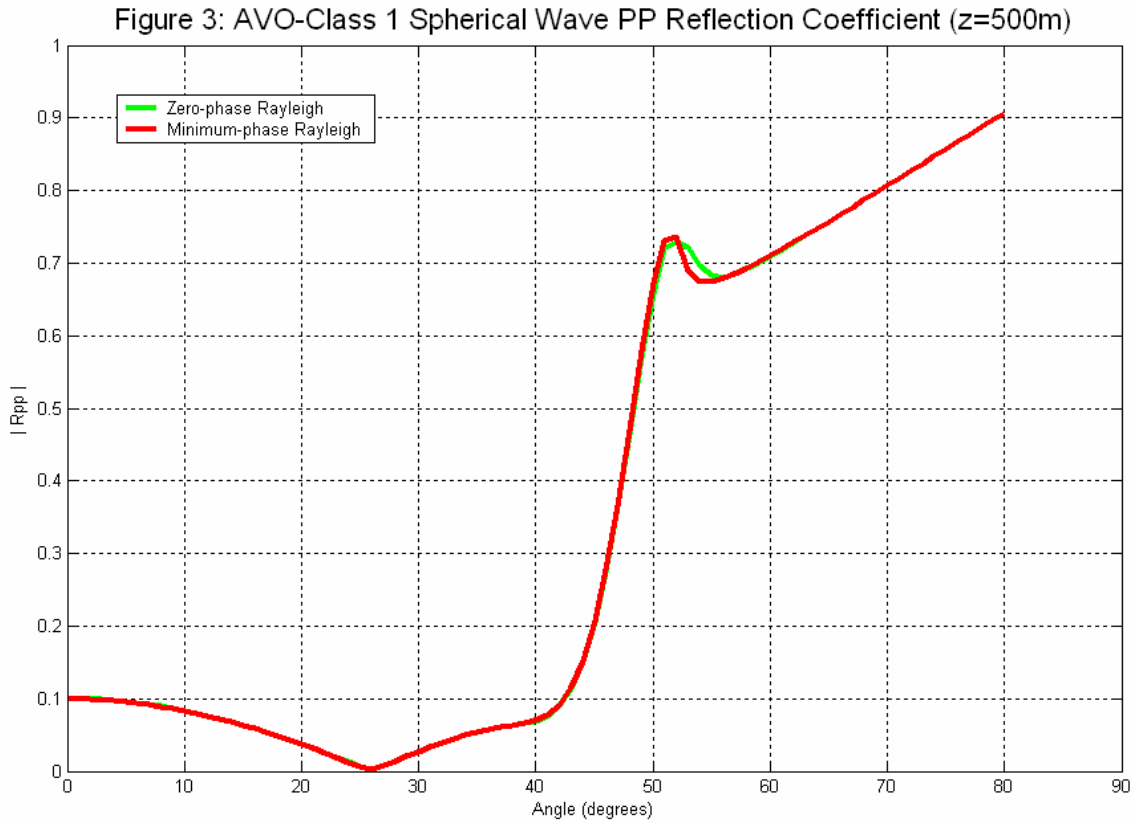


FIG. 3: Spherical-wave reflection coefficient curves for two different Rayleigh wavelets which share the same amplitude spectrum but differ in phase.

DISCUSSION

The results show clearly that spherical-wave reflection coefficients beyond the critical angle do depend on phase specification. The changes do not affect the overall shape of the reflectivity curve, but do modify its behavior in this post-critical region.

To understand this difference in behavior, we can look at the weighting functions, which, for general wavelets, are given by equation 3. In Figure 4 we show the weighting functions for the zero-phase and minimum-phase Ormsby wavelets. The angle of incidence is specified as $\theta_i = 40^\circ$ and the function is plotted against the integration parameter θ . The main central lobes of the real (a) and imaginary (b) parts are similar for the two wavelets, but the tail regions are more extended and oscillatory for the zero-phase wavelet. In Figure 5 we show the same functions but for the Rayleigh wavelet. In this case, there is again more difference in the tails, but neither is markedly extended beyond the other.

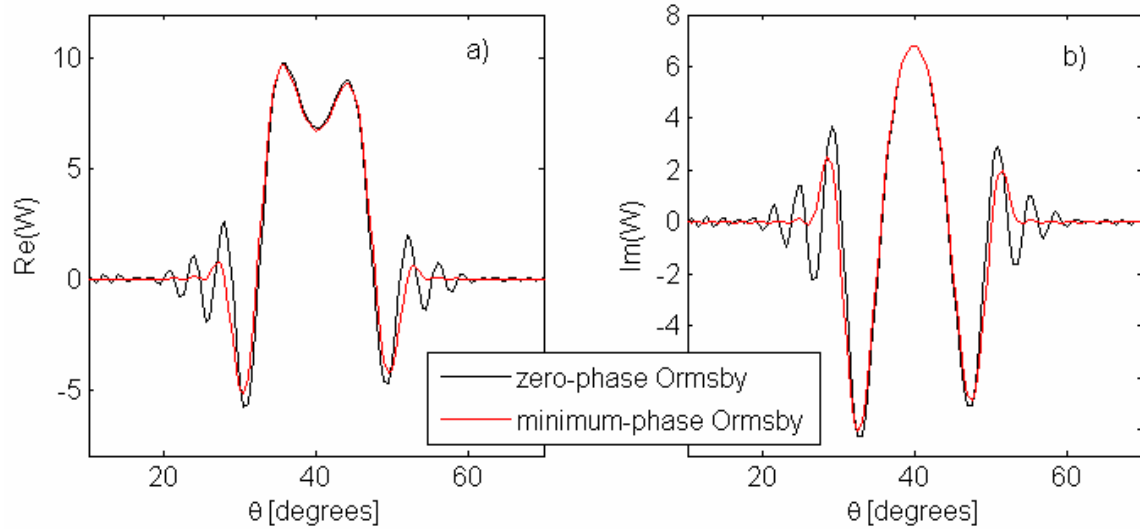


FIG. 4: Weighting functions for Ormsby wavelets calculated using equation 3. The red line represents the result using a minimum-phase wavelet, and the black line the zero-phase. Real components are shown in a) and imaginary components in b).

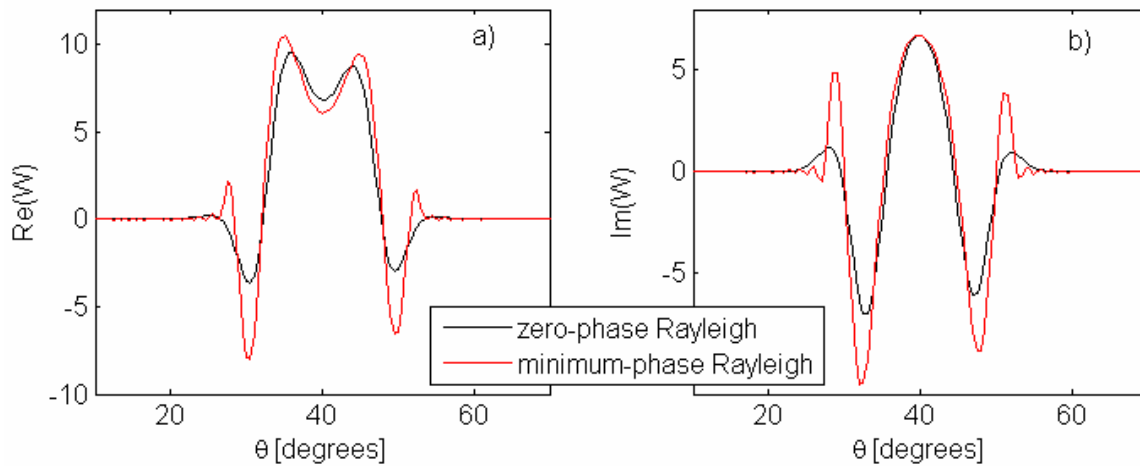


FIG. 5: Weighting functions for Rayleigh wavelets calculated using equation 3. The red line represents the result using a minimum-phase wavelet, and the black line the zero-phase. Real components are shown in a) and imaginary components in b).

We note that the main lobe is similar for both the Ormsby and Rayleigh wavelets. This part of the function is likely determined by the average frequency, which is 50 Hz for both wavelets. We show in Figure 6a the variation of $|W|$ with f_0 , and in Figure 6b the variation with n , for Rayleigh wavelets in both cases. This shows that the lobe height is most strongly influenced by f_0 , and that the influence of n is mostly on the wings.

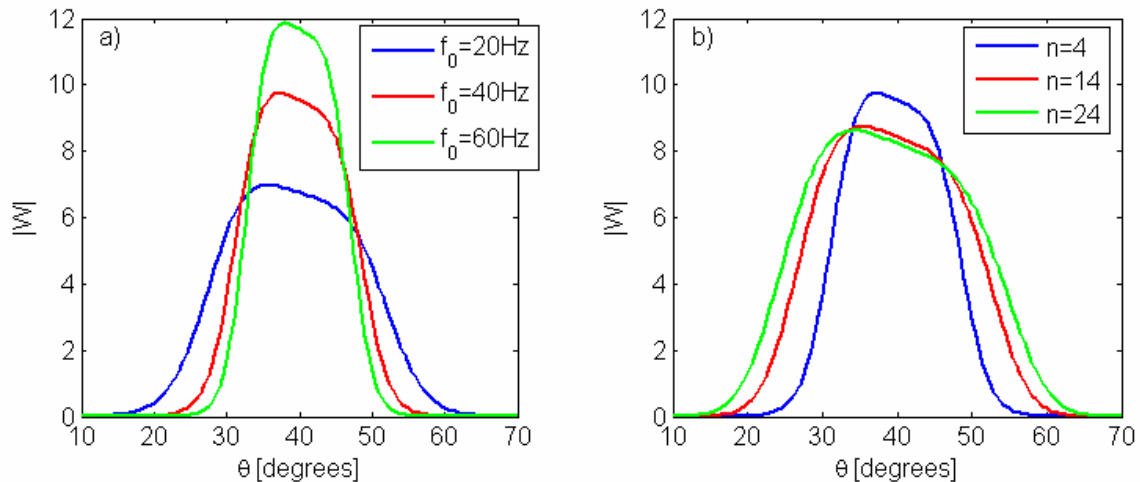


FIG. 6: The envelope of the weighting function W for Rayleigh wavelets. a) Variation with f_0 (with $n = 4$). b) Variation with n (with $f_0 = 40$ Hz). Note that both parts have the same vertical scale

We have seen in another report in this volume (Ursenbach & Haase, 2006) that extended, oscillatory tails in the weighting function are associated with post-critical oscillations in the reflectivity curve, both for monochromatic waves, and for narrow-band Rayleigh wavelets. In this present study all the wavelets considered are reasonably wide-band, but one of them, the zero-phase Ormsby, has notably sharp slope discontinuities. Thus smooth, wide-band wavelets appear to yield spherical-wave reflection coefficients which sample a compact range of plane-wave reflection coefficients, while wavelets with narrow or jagged bands sample a wider range of plane-wave coefficients and do so less smoothly.

CONCLUSIONS

Spherical-wave reflection coefficients can vary with wavelet phase, even if the amplitude is held constant. Constant-phase and linear-phase results do not differ from those for zero-phase, but minimum-phase wavelets do yield different reflection coefficients in a region just above the critical angle. The overall trend of the reflectivity curve is not affected, so that the differences may not be critical in applications to seismic exploration.

Spherical-wave reflection coefficients are weighted integrals of plane-wave reflection coefficients, and the differing results described above result from different weighting functions. Thus the formulation of spherical-wave reflection coefficients in terms of weighting functions helps to provide insight into post-critical behavior.

ACKNOWLEDGEMENTS

The authors wish to thank the Sponsors of CREWES for support of this research.

REFERENCES

- Haase, A. B., 2004, Spherical wave AVO modeling of converted waves in elastic isotropic media: 2004 CSEG National Convention.
- Ursenbach, C. P. and Haase, A. B., 2004, An efficient method for calculating spherical-wave reflection coefficients, CREWES Research Report, **16**.
- Ursenbach, C. P. and Haase, A. B., 2006, AVO modeling of monochromatic spherical waves: comparison to band-limited waves, CREWES Research Report, **18**.

APPENDIX

From equation 1 and the subsequent discussion we begin by writing the spherical-wave reflection coefficient as

$$R_{PP}^{\text{spherical}}(\theta_i) = \frac{u}{u_{R_{PP}=1}}$$

$$= \frac{\int_0^\infty w(\omega) e^{-i\omega t} \left[i\omega^2 \int_0^\infty \frac{p}{\xi} R_{PP}(p) [-pJ_1(\omega pr) \sin \theta_i + i\xi J_0(\omega pr) \cos \theta_i] \exp[i\omega\xi(z+h)] dp \right] d\omega}{\int_0^\infty w(\omega) e^{-i\omega t} \left[\left(-\frac{1}{R^2} + \frac{i\omega}{R\alpha_1} \right) \exp\left(i\frac{\omega R}{\alpha_1} \right) \right] d\omega}.$$

Setting $t = R/\alpha_1 + t_{\text{shift}}$, and reversing the order of integration yields

$$R_{PP}^{\text{spherical}}(\theta_i) =$$

$$= \frac{\int_0^\infty \frac{p}{\xi} R_{PP}(p) \left[i \int_0^\infty w(\omega) \omega^2 [-pJ_1(\omega pr) \sin \theta_i + i\xi J_0(\omega pr) \cos \theta_i] \exp\{i\omega[\xi(z+h) - R/\alpha_1 - t_{\text{shift}}]\} d\omega \right] dp}{\int_0^\infty w(\omega) e^{-i\omega t_{\text{shift}}} \left(-\frac{1}{R^2} + \frac{i\omega}{R\alpha_1} \right) d\omega}.$$

Finally we change the variable of the p -integration to $\cos\theta$. Thus the differential $(p/\xi)dp$ becomes $[-d(\cos\theta)/\alpha_1]$, and W may then be extracted by comparison with equation 2.